Chaos, Solitons and Fractals 182 (2024) 114814

Contents lists available at ScienceDirect

Chaos, Solitons and Fractals

journal homepage: www.elsevier.com/locate/chaos

Dynamic event-triggered adaptive tracking control for stochastic nonlinear systems with deferred time-varying constraints ☆

Dong-Mei Wang [a], Yu-Qun Han [a,b], Li-Ting Lu [a], Shan-Liang Zhu [a,b,c,*]

[a] School of Mathematics and Physics, Qingdao University of Science and Technology, Qingdao 266061, China
[b] Qingdao Innovation Center of Artificial Intelligence Ocean Technology, Qingdao 266061, China
[c] The Research Institute for Mathematics and Interdisciplinary Sciences, Qingdao University of Science and Technology, Qingdao 266061, China

ARTICLE INFO

Keywords:
Event-triggered control
Adaptive control
Multi-dimensional Taylor network
Deferred time-varying constraints
Stochastic nonlinear systems

ABSTRACT

This article investigates the problem of adaptive tracking control for stochastic nonlinear systems with deferred state constraints. The novel unified universal barrier function (UUBF) and deferred funnel error transformation are developed to handle various state constraints and adjust the tracking error more precisely, respectively. Multi-dimensional Taylor network (MTN) and dynamic event-triggered mechanism (DETM) are employed to design controller in the backstepping process, which can achieve full-state constraints and the tracking control after the preassigned time while conserving more communication resources. Finally, two simulation examples are presented to verify the effectiveness of the proposed control scheme.

1. Introduction

It is well known that many practical systems are subject to stochastic disturbances [1,2], which are not negligible factors leading to system instability. In this context, research on adaptive control of stochastic nonlinear systems has continued from decades ago to the present and a lot of valuable results have been produced [3–8]. Dealing with unknown nonlinear terms is a key challenge that needs to be tackled during the controller design process. Multi-dimensional Taylor network (MTN) [9], which plays the same role as neural network [10–12] and fuzzy logic system [13,14], is a popular method used to approximate unknown nonlinear functions. Moreover, MTN method and adaptive backstepping method have been employed to co-design controllers for different types of controlled systems, such as switched nonlinear systems with prescribed performance [15] or with multiple objective constraints [16], stochastic nonlinear systems with multiple faults [17] or with time-varying delays [18], and stochastic nonlinear discrete-time systems with time-varying delays [19]. However, these aforementioned results did not take deferred time-varying constraints and limited network resources into account.

Due to physical constraints or performance requirements, many practical controlled systems operate under certain constraints, which has attracted research interest in the control field over the last few decades. Existing research results have been mainly categorized into output constraints [20–23] and state constraints [24–27]. However, the barrier Lyapunov functions designed in these articles were based on the conservative assumption that the constraints were imposed at the beginning of system operation, which implies that the initial conditions must satisfy the given boundary functions. Many scholars have made some efforts to find solutions to relax this assumption. In case of nonlinear systems with completely unknown initial conditions, the authors in [28] proposed deferred asymmetric time-varying full-state constraints which mean that the state constraints can be imposed after the system has been running for a period of time. Subsequently, the authors in [29,30] developed event-triggered adaptive control schemes for multiagent systems with deferred constraints and nonlinear systems with deferred output constraint, respectively. The authors in [31] investigated the problem of fault-tolerant control for stochastic systems with deferred output constraint. Regrettably, when the two boundary functions do not satisfy one being positive and the other being negative, the proposed control schemes mentioned above are ineffective. Recently, the authors in [32] constructed an improved unified universal barrier function (UUBF) to deal with this problem. However, there are few studies on stochastic nonlinear systems with deferred time-varying constraints owing to its complexity, which inspires us to take on the challenge.

In recent years, with the development of network communication technology, it has become a trend to establish network communication transmission between controlled systems and factories in practical production. Reducing communication transmission while ensuring control performance is an issue that needs to be studied in view of

☆ This work was supported by the Shandong Provincial Natural Science Foundation, China (No. ZR2020QF055).

* Corresponding author at: School of Mathematics and Physics, Qingdao University of Science and Technology, Qingdao 266061, China.
E-mail address: zhushanliang@qust.edu.cn (S.-L. Zhu).

https://doi.org/10.1016/j.chaos.2024.114814
Received 2 January 2024; Received in revised form 1 March 2024; Accepted 25 March 2024
Available online 3 April 2024
0960-0779/

the limited network resources. The authors in [33] suggested that event-triggered mechanism (ETM) can effectively address this issue. Afterwards, ETM-based control approaches have been widely used in various systems thanks to its unique dominance in saving communication resources [34–37]. It is worth noting that the threshold parameter of ETM has a direct impact on both the data transmission frequency and data transmission volume. Hence, it is especially crucial to design the ETM with dynamically adjustable threshold. The author in [38] proposed a dynamic event-triggered mechanism (DETM) for the first time by including an internal dynamic variable in the design process of ETM. The DETM can adjust the event-triggered threshold flexibly with the change of system states, which effectively improves the efficiency of resource utilization and system control performance. As a result, this mechanism has been applied to design controllers of nonlinear systems [39–41] and uncertain stochastic nonlinear systems [42]. Nevertheless, a little research has been done on DETM-based control for stochastic nonlinear systems with deferred time-varying constraints, which motivates us to carry out this work.

Based on the aforementioned results, this article develops a novel DETM-based adaptive controller for stochastic nonlinear systems with deferred time-varying state constraints. In comparison with the existing results, the highlights of this article are summarized below:

(1) This article is the first to investigate the tracking control problem of stochastic nonlinear systems with deferred time-varying constraints by means of DETM and MTN method. The improved shifting function and UUBF can relax the constraints on initial conditions of the system and widen the scope of selection for boundary functions. In contrast to previous results about nonlinear systems with deferred constraints [28,30], the proposed control scheme is more applicable in practical contexts.

(2) A novel deferred funnel error transformation is developed to make the tracking error converge to a prescribed region after the preassigned time. Moreover, the preassigned time is irrelevant to the designed controller parameters and initial conditions so that it can be adjusted based on practical requirements. Hence, the proposed control scheme can enhance the transient and steady-state performance of the controlled system.

(3) A new coordinate transformation involving nonlinear mappings is introduced to simplify the design of Lyapunov functions. Furthermore, the DETM is utilized to improve the responsiveness of the system by updating event-triggered condition in real-time. Therefore, the designed controller has a simple structure and can economize more communication resources than the event-triggered controller designed in [43].

2. Preliminaries and formulation

The following notations will be used consistently in this article.

Notations: R and R^i denote the set of real numbers and the i-dimensional real space, respectively. $R^{n\times r}$ denotes the space of $n \times r$ matrices with real numbers. The superscript T is defined as the transpose of a vector or a matrix. $\|\cdot\|$ represents the Euclidean norm. A function is called C^2 function, which indicates that it is 2-times continuously differentiable. A continuous and strictly increasing function $x(t)$ is belong to $\mathcal{K}_\infty$ class functions if $x(t) \to \infty$ as $t \to \infty$.

2.1. Control object and objective

In this article, the following class of state-feedback stochastic nonlinear system with deferred time-varying constraints is investigated:

$$\begin{cases} d\zeta_i = \left(\zeta_{i+1} + f_i\left(\bar{\zeta}_i\right)\right)dt + g_i^{\mathrm{T}}\left(\bar{\zeta}_i\right)d\omega \\ d\zeta_n = \left(u + f_n\left(\bar{\zeta}_n\right)\right)dt + g_n^{\mathrm{T}}\left(\bar{\zeta}_n\right)d\omega \\ \quad y = \zeta_1, i = 1, \dots, n-1 \end{cases} \tag{1}$$

where $\zeta_i \in R$ denotes the system state and $\bar{\zeta}_i = [\zeta_1, \dots, \zeta_i]^{\mathrm{T}} \in R^i, i = 1, 2, \dots, n$. $u \in R$ and $y \in R$ stand for the control input and the system output, respectively. ω represents an independent r-dimensional standard Brownian motion. $f_i\left(\bar{\zeta}_i\right) \in R$ and $g_i\left(\bar{\zeta}_i\right) \in R^r$ represent unknown smooth nonlinear functions satisfying $f_i(\mathbf{0}) = 0$ and $g_i(\mathbf{0}) = \mathbf{0}$.

As a matter of fact, many engineering systems are subject to deferred state constraints. It means that all of the system states are unconstrained on an initial interval, and then they are constrained to a bounded region starting from $t = T_p > 0$, where T_p denotes the preassigned time. Specifically, it is expressed as follows:

(1) Each state ζ_i of system (1) is not subject to any constraints when the time t is within the interval $\left[0, T_p\right)$.

(2) ζ_i is constrained on the time interval $\left[T_p, \infty\right)$, which can be described as

$$\zeta_i \in \Omega_i = \left\{\zeta_i \in R \mid -\kappa_{iL} < \zeta_i < \kappa_{iR}\right\} \tag{2}$$

where κ_{iL} and κ_{iR} are known time-varying boundary functions satisfying $-\kappa_{iL} < \kappa_{iR}$. Moreover, κ_{iL}, κ_{iR}, $\dot{\kappa}_{iL}$, $\dot{\kappa}_{iR}$, $\ddot{\kappa}_{iL}$ and $\ddot{\kappa}_{iR}$ are continuous and bounded.

Remark 1. An intuitive example involving such deferred constraints is that a mobile robot starts in a free-moving region for a period of time (preassigned time) and then it enters a narrower region (constrained) to avoid collisions. In addition, the preassigned time T_p is irrelevant to the designed controller parameters and initial conditions, which can be set precisely in accordance with practical requirements.

Control Objective: Develop a DETM-based adaptive tracking control scheme for the controlled stochastic system (1) such that: (i) all the signals of the controlled system are implemented as SGUUB in the sense of 4th moment. (ii) after the preassigned time T_p, all system states strictly obey the pregiven boundary constraints and the tracking error $e_1 = \zeta_1 - y_r$ converges to a prescribed region, where y_r denotes the tracking expectation signal.

Assumption 1. The tracking expectation signal y_r and its ith-order derivatives $y_r^{(i)}(i = 1, \dots, n)$ are piecewise continuous, known, and bounded. In order to implement the full-state constraints, y_r needs to satisfy $-\kappa_{1L} < y_r < \kappa_{1R}$ after the preassigned time T_p.

2.2. Stochastic systems theory

To introduce the definitions and theorems of stochastic nonlinear systems, take the following general stochastic system into account:

$$d\zeta = \Phi(\zeta)dt + \Psi(\zeta)d\omega \tag{3}$$

where $\zeta \in R^n$ denotes the state vector, ω represents an independent r-dimensional standard Brownian motion. $\Phi(\cdot) : R^n \to R^n$ and $\Psi(\cdot) : R^n \to R^{n\times r}$ are locally Lipschitz functions satisfying $\Phi(\mathbf{0}) = \mathbf{0} \in R^n$ and $\Psi(\mathbf{0}) = \mathbf{0} \in R^{n\times r}$.

Definition 1 (*[44]*). For any given $V(\zeta)$ with continuous second-order partial derivative, $LV(\zeta)$ denotes the differential operator of $V(\zeta)$ relating to the stochastic system (3) and dV denotes the derivative of V. LV and dV are defined as the following forms

$$LV(\zeta) = \frac{\partial V(\zeta)}{\partial \zeta}\Phi(\zeta) + \frac{1}{2}Tr\left\{\Psi^{\mathrm{T}}(\zeta)\frac{\partial^2 V(\zeta)}{\partial \zeta^2}\Psi(\zeta)\right\} \tag{4}$$

$$dV(\zeta) = LV(\zeta)dt + \frac{\partial V(\zeta)}{\partial \zeta}\Psi(\zeta)d\omega \tag{5}$$

where $Tr\{\cdot\}$ stands for the trace of $\cdot$.

Lemma 1 (*[34]*). *For* $\forall\nabla \in R$ *and* $\delta > 0$, *one can get the inequality:* $0 \le |\nabla| - \nabla\tanh\left(\frac{\nabla}{\delta}\right) \le 0.2785\delta$.

Lemma 2 ([42]). *For the stochastic system (3), if there exists a positive definite function $V(\zeta) \in C^2$, $\mathcal{K}_\infty$ class functions Υ_1 and Υ_2, and real numbers $b > 0$ and $\Xi > 0$, such that the following two inequalities hold*

$$\begin{aligned} &\Upsilon_1(\|\zeta\|) \le V(\zeta) \le \Upsilon_2(\|\zeta\|) \\ &LV(\zeta) \le -bV(\zeta) + \Xi \end{aligned} \tag{6}$$

After that, the system (3) has a unique solution satisfying

$$E[V(\zeta)] \le V(\zeta_0)e^{-bt} + \frac{\Xi}{b} \tag{7}$$

where $E[V(\zeta)]$ denotes the mathematical expectation of $V(\zeta)$.

Definition 2 ([42]). The trajectory $\{\zeta(t), t \ge 0\}$ of stochastic system (3) is considered to be semi-globally uniformly ultimately bounded (SGUUB) in the sense of pth moment, if for a compact set $\Theta \in R^n$ and any initial state $\zeta(t_0) = \zeta_0 \in \Theta$, there exists a constant $\psi > 0$ and a time constant $T_c = T_c(\psi, \zeta_0)$ such that $E(\|\zeta(t)\|^p) < \psi$ for any $t > t_0 + T_c$.

2.3. Multi-dimensional Taylor network

As a neural network characterized by a simple structure, MTN possesses effective nonlinear approximation capabilities. Given that stochastic systems contain unknown nonlinear terms, MTN is utilized to approximate these unknown terms as the following Lemma.

Lemma 3 ([15]). *Assume $H(\zeta): R^n \to R$ is a continuous nonlinear function which is defined on a compact set Ω, then for $\forall \bar{\varepsilon} > 0$, $H(\zeta)$ can be approximated with the aid of $\boldsymbol{W}^{\mathrm{T}} S_{m_n}(\zeta)$ as follows:*

$$H(\zeta) = \boldsymbol{W}^{\mathrm{T}} S_{m_n}(\zeta) + \varepsilon(\zeta), |\varepsilon(\zeta)| \le \bar{\varepsilon} \tag{8}$$

where $S_{m_n}(\zeta) = \left[\zeta_1, \zeta_2, \dots, \zeta_n, \zeta_1^2, \zeta_1\zeta_2, \dots, \zeta_n^2, \dots, \zeta_1^m, \dots, \zeta_n^m\right]^{\mathrm{T}} \in R^k$ represents the middle layer of MTN. $\boldsymbol{W} = [W_1, W_2, \dots, W_k]^{\mathrm{T}} \in R^k$ and $\boldsymbol{\zeta} = [\zeta_1, \zeta_2, \dots, \zeta_n]^{\mathrm{T}} \in R^n$ stand for the weight vector and input vector of MTN, respectively. $\varepsilon(\zeta) \in R$ represents the approximation error of MTN.

Remark 2. MTN is a network structure similar to radial basis function neural network (RBFNN) [10]. In contrast to RBFNN, its structure is simpler because polynomials are adopted instead of radial basis functions in the middle layer of MTN. Moreover, MTN can realize the fast approximation of nonlinear functions with less computation [17,18].

2.4. Dynamic event-triggered mechanism

The DETM is applied to reduce the communication burden in the controller-to-actuator channel. Using the same design approach as [42], the DETM is described as the following form

$$u(t) = \varpi(t_k), \forall t \in [t_k, t_{k+1}), k \in Z^+ \tag{9}$$

$$\begin{cases} t_{k+1} = \inf\{t \,\|\, \varrho(t) \,| \ge \iota + \varsigma\} \\ \dot{\varsigma} = -a\varsigma + (\iota - |\varrho(t)|) \end{cases} \tag{10}$$

where ι and a denote positive design constants. $\varrho(t) = u(t) - \varpi(t)$ is the measurement error, and ς represents an internal dynamic variable.

Remark 3. The proposed DETM can be accurately triggered according to the event-triggered condition, avoiding the waste of communication resources. In contrast to ETM in [43], the DETM can extend the interval between two adjacent events by a dynamically changing parameter, resulting in greater conservation of communication resources [38].

3. Control design and stability analysis

3.1. Unified universal barrier function

In order to expand the choice of boundary functions, similar to [32], an improved shifting function is constructed as follows:

$$X_i = \beta(t)\zeta_i + \rho(t)\kappa_{Mi} \tag{11}$$

where $\kappa_{Mi} = \frac{1}{2}(\kappa_{iR} - \kappa_{iL})$ represents the intermediate function consisting of the upper function κ_{iR} and the lower boundary function $-\kappa_{iL}$. Both $\beta(t)$ and $\rho(t)$ denote shifting functions defined as follows:

$$\beta(t) = \begin{cases} \left(\sin\left(\frac{\pi t}{2T_p}\right)\right)^n, & 0 \le t < T_p \\ 1, & t \ge T_p \end{cases} \tag{12}$$

$$\rho(t) = \begin{cases} \left(\frac{T_p - t}{T_p}\right)^{(n+1)}, & 0 \le t < T_p \\ 0, & t \ge T_p \end{cases} \tag{13}$$

where T_p represents the preassigned time and n denotes the amount of system state variables.

Motivated by [26], to ensure all the states of the controlled system (1) satisfy different types of boundary constraints, a novel UUBF is constructed with the aid of the newly designed function X_i in the following form

$$\gamma_i = \frac{(\kappa_{Mi} + \kappa_{iL})(\kappa_{iR} - \kappa_{Mi})(X_i - \kappa_{Mi})}{(X_i + \kappa_{iL})(\kappa_{iR} - X_i)}. \tag{14}$$

3.2. Coordinate transformation

A finite-time performance function in [45] as a funnel function is introduced, which is specified as follows:

$$\varphi(t) = \begin{cases} \left(\varphi_0 - \frac{t}{T_p}\right)e^{1 - \frac{T_p}{T_p - t}} + \varphi_1, & 0 \le t < T_p \\ \varphi_1, & t \ge T_p \end{cases} \tag{15}$$

where T_p represents the preassigned time. φ_0 and φ_1 are positive design constants.

In order to relax the constraints on the initial values and adjust the tracking error more flexibly, the finite-time performance function φ and the shift function β are applied to co-design the novel deferred funnel error transformation in the following form

$$\tau_1 = \frac{\beta e_1}{\sqrt{\varphi^2 - (\beta e_1)^2}} \tag{16}$$

where $e_1 = \zeta_1 - y_r$ denotes the tracking error.

To ease the subsequent design of Lyapunov functions, the coordinate transformation with nonlinear mappings is presented as follows:

$$\begin{cases} Z_1 = S_1 \\ Z_i = S_i - \alpha_{i-1}, i = 2, \dots, n \end{cases} \tag{17}$$

where $S_1 = \beta\tau_1$, $S_i = \beta\gamma_i$, and α_{i-1} will be defined in the process of backstepping.

In view of Definition 1 and (11)–(17), it is not hard to obtain that the following equations hold:

$$de_1 = F_{e_1}dt + G_{e_1}d\omega \tag{18}$$

where $F_{e_1} = \zeta_2 + f_1(\bar{\zeta}_1) - \dot{y}_r$ and $G_{e_1} = g_1^{\mathrm{T}}(\bar{\zeta}_1)$.

$$d\tau_1 = F_{\tau_1}dt + G_{\tau_1}d\omega \tag{19}$$

where $F_{\tau_1} = \frac{\partial\tau_1}{\partial e_1}F_{e_1} + \frac{1}{2}\frac{\partial^2\tau_1}{\partial e_1^2}G_{e_1}^{\mathrm{T}}G_{e_1} + \frac{\partial\tau_1}{\partial t}$, $G_{\tau_1} = \frac{\partial\tau_1}{\partial e_1}G_{e_1}$.

$$\begin{aligned} dX_i &= \left(\beta\zeta_{i+1} + \beta f_i + \dot{\beta}\zeta_i + \dot{\rho}\kappa_{Mi} + \rho\dot{\kappa}_{Mi}\right)dt + \left(\beta g_i^{\mathrm{T}}\right)d\omega \\ &= F_{X_i}dt + G_{X_i}d\omega \end{aligned} \tag{20}$$

where $F_{X_i} = \beta\zeta_{i+1} + \beta f_i + \dot{\beta}\zeta_i + \dot{\rho}\kappa_{Mi} + \rho\dot{\kappa}_{Mi}$ and $G_{X_i} = \beta g_i^{\mathrm{T}}$.

$$d\gamma_i = F_{\gamma_i}dt + G_{\gamma_i}d\omega \tag{21}$$

where $F_{\gamma_i} = \frac{\partial\gamma_i}{\partial X_i}F_{X_i} + \frac{1}{2}\frac{\partial^2\gamma_i}{\partial X_i^2}G_{X_i}^{\mathrm{T}}G_{X_i} + \frac{\partial\gamma_i}{\partial t}$, $G_{\gamma_i} = \frac{\partial\gamma_i}{\partial X_i}G_{X_i}$.

$$dS_1 = F_{S_1}dt + G_{S_1}d\omega \tag{22}$$

where $F_{S_1} = \frac{\partial S_1}{\partial\tau_1}F_{\tau_1} + \frac{1}{2}\frac{\partial^2 S_1}{\partial\tau_1^2}G_{\tau_1}^{\mathrm{T}}G_{\tau_1} + \frac{\partial S_1}{\partial t}$, $G_{S_1} = \beta\frac{\partial S_1}{\partial\tau_1}G_{\tau_1}$.

$$dS_i = F_{S_i}dt + G_{S_i}d\omega \tag{23}$$

where $i = 2, \dots, n$ and $F_{S_i} = \frac{\partial S_i}{\partial\gamma_i}F_{\gamma_i} + \frac{1}{2}\frac{\partial^2 S_i}{\partial\gamma_i^2}G_{\gamma_i}^{\mathrm{T}}G_{\gamma_i} + \frac{\partial S_i}{\partial t}$, $G_{S_i} = \beta\frac{\partial S_i}{\partial\gamma_i}G_{\gamma_i}$.

According to the nonlinear mapping relations in [46], the coordinate transformation (17) and (22)–(23), the controlled system (1) can be converted into the following new system

$$\begin{cases} dS_i = \left(S_{i+1} + \bar{F}_{S_i}\right)dt + G_{S_i}d\omega \\ dS_n = \left(u + \bar{F}_{S_n}\right)dt + G_{S_n}d\omega \end{cases} \tag{24}$$

where $i = 1, \dots, n-1$, $\bar{F}_{S_i} = F_{S_i} - S_{i+1}$, and $\bar{F}_{S_n} = F_{S_n} - u$.

3.3. DETM-based controller design and stability analysis

Step 1*:* The first candidate Lyapunov function is constructed as follows:

$$V_1 = \frac{1}{4}Z_1^4 + \frac{1}{2}\tilde{\boldsymbol{W}}_1^{\mathrm{T}}\boldsymbol{\Gamma}_1^{-1}\tilde{\boldsymbol{W}}_1 \tag{25}$$

where $\boldsymbol{\Gamma}_1 = \boldsymbol{\Gamma}_1^{\mathrm{T}} > 0$ stands for a constant matrix. $\hat{\boldsymbol{W}}_1$ denotes the estimate of unknown parameter $\boldsymbol{W}_1$. $\tilde{\boldsymbol{W}}_1 = \boldsymbol{W}_1 - \hat{\boldsymbol{W}}_1$ represents the parameter estimate error.

According to the coordinate transformation (17), we have $Z_1 = S_1$ and $S_2 = Z_2 + \alpha_1$. Then, based on Definition 1 and (24)–(25), the differential operator of V_1 is given in the following form

$$\begin{aligned} LV_1 &= Z_1^3\left(S_2 + \bar{F}_{S_1}\right) + \frac{3}{2}Z_1^2G_{S_1}^{\mathrm{T}}G_{S_1} - \tilde{\boldsymbol{W}}_1^{\mathrm{T}}\boldsymbol{\Gamma}_1^{-1}\dot{\hat{\boldsymbol{W}}}_1 \\ &= Z_1^3\left(Z_2 + \alpha_1 + \bar{F}_{S_1}\right) + \frac{3}{2}Z_1^2G_{S_1}^{\mathrm{T}}G_{S_1} - \tilde{\boldsymbol{W}}_1^{\mathrm{T}}\boldsymbol{\Gamma}_1^{-1}\dot{\hat{\boldsymbol{W}}}_1. \end{aligned} \tag{26}$$

With the aid of Young's inequality, it is not hard to obtain the following two inequalities hold

$$Z_1^3Z_2 \le \frac{3}{4}Z_1^4 + \frac{1}{4}Z_2^4 \tag{27}$$

$$\frac{3}{2}Z_1^2G_{S_1}^{\mathrm{T}}G_{S_1} \le \frac{3}{4l_1^2}Z_1^4\left\|G_{S_1}\right\|^4 + \frac{3}{4}l_1^2 \tag{28}$$

where l_1 denotes a positive constant.

Substituting (27) and (28) into (26), one has

$$LV_1 \le Z_1^3\left(\alpha_1 + H_1\right) + \frac{1}{4}Z_2^4 + \frac{3}{4}l_1^2 - \tilde{\boldsymbol{W}}_1^{\mathrm{T}}\boldsymbol{\Gamma}_1^{-1}\dot{\hat{\boldsymbol{W}}}_1 \tag{29}$$

where $H_1 = \bar{F}_{S_1} + \frac{3}{4}Z_1 + \frac{3}{4l_1^2}Z_1\left\|G_{S_1}\right\|^4$. Obviously, H_1 cannot be used to design controller because it contains unknown functions. By introducing Lemma 3, MTN is employed to approximate the unknown function H_1. Specifically, for $\forall\bar{\varepsilon}_1 > 0$, there is a MTN as $\boldsymbol{W}_1^{\mathrm{T}}S_{m_1}(\boldsymbol{z}_1)$, such that

$$H_1 = \boldsymbol{W}_1^{\mathrm{T}}S_{m_1}(\boldsymbol{z}_1) + \varepsilon_1(\boldsymbol{z}_1), \left|\varepsilon_1(\boldsymbol{z}_1)\right| \le \bar{\varepsilon}_1 \tag{30}$$

where $\boldsymbol{z}_1 = \left[Z_1\right]^{\mathrm{T}}$. $\varepsilon_1(\boldsymbol{z}_1)$ represents the approximation error.

Using Young's inequality again, one obtains

$$Z_1^3\varepsilon_1(\boldsymbol{z}_1) \le \frac{3}{4}Z_1^4 + \frac{1}{4}\bar{\varepsilon}_1^4. \tag{31}$$

Next, combining (30) and (31), (29) can be expressed in the following form

$$\begin{aligned} LV_1 \le& Z_1^3\left(\alpha_1 + \boldsymbol{W}_1^{\mathrm{T}}S_{m_1}\right) + \frac{1}{4}Z_2^4 + \frac{3}{4}Z_1^4 \\ &+ \frac{3}{4}l_1^2 - \tilde{\boldsymbol{W}}_1^{\mathrm{T}}\boldsymbol{\Gamma}_1^{-1}\dot{\hat{\boldsymbol{W}}}_1 + \frac{1}{4}\bar{\varepsilon}_1^4. \end{aligned} \tag{32}$$

In order to achieve the proposed control objectives, the virtual control signal α_1 and the adaptive law $\dot{\hat{\boldsymbol{W}}}_1$ are designed as

$$\alpha_1 = -c_1Z_1 - \frac{3}{4}Z_1 - \hat{\boldsymbol{W}}_1^{\mathrm{T}}S_{m_1} \tag{33}$$

$$\dot{\hat{\boldsymbol{W}}}_1 = \boldsymbol{\Gamma}_1\left(S_{m_1}Z_1^3 - \sigma_1\hat{\boldsymbol{W}}_1\right) \tag{34}$$

where c_1 and σ_1 represent positive design constants.

Substituting (33)–(34) into (32), a new form of the differential operator of V_1 can be described as

$$LV_1 \le -c_1Z_1^4 + \frac{1}{4}Z_2^4 + \frac{1}{4}\bar{\varepsilon}_1^4 + \frac{3}{4}l_1^2 + \sigma_1\tilde{\boldsymbol{W}}_1^{\mathrm{T}}\hat{\boldsymbol{W}}_1. \tag{35}$$

Step i $(2 \le i \le n-1)$*:* Construct the ith candidate Lyapunov function, the specific form of which is as follows:

$$V_i = V_{i-1} + \frac{1}{4}Z_i^4 + \frac{1}{2}\tilde{\boldsymbol{W}}_i^{\mathrm{T}}\boldsymbol{\Gamma}_i^{-1}\tilde{\boldsymbol{W}}_i \tag{36}$$

where $\boldsymbol{\Gamma}_i = \boldsymbol{\Gamma}_i^{\mathrm{T}} > 0$ stands for a constant matrix. $\hat{\boldsymbol{W}}_i$ denotes the estimate of unknown parameter $\boldsymbol{W}_i$. $\tilde{\boldsymbol{W}}_i = \boldsymbol{W}_i - \hat{\boldsymbol{W}}_i$ represents the parameter estimate error.

According to the coordinate transformation (17), we have $Z_i = S_i - \alpha_{i-1}$ and $S_{i+1} = Z_{i+1} + \alpha_i$. Then, based on Definition 1 and (36), the differential operator of V_i can be expressed as

$$\begin{aligned} LV_i =& LV_{i-1} + Z_i^3\left(S_{i+1} + \bar{F}_{S_i} - L\alpha_{i-1}\right) + \frac{3}{2}Z_i^2\bar{G}_{S_i}^{\mathrm{T}}\bar{G}_{S_i} - \tilde{\boldsymbol{W}}_i^{\mathrm{T}}\boldsymbol{\Gamma}_i^{-1}\dot{\hat{\boldsymbol{W}}}_i \\ =& LV_{i-1} + Z_i^3\left(Z_{i+1} + \alpha_i + \bar{F}_{S_i} - L\alpha_{i-1}\right) \\ &+ \frac{3}{2}Z_i^2\bar{G}_{S_i}^{\mathrm{T}}\bar{G}_{S_i} - \tilde{\boldsymbol{W}}_i^{\mathrm{T}}\boldsymbol{\Gamma}_i^{-1}\dot{\hat{\boldsymbol{W}}}_i \end{aligned} \tag{37}$$

where $\bar{G}_{S_i} = G_{S_i} - \sum_{j=1}^{i-1}\frac{\partial\alpha_{i-1}}{\partial S_j}G_{S_j}$, $L\alpha_{i-1} = \sum_{j=1}^{i-1}\frac{\partial\alpha_{i-1}}{\partial\hat{\boldsymbol{W}}_j}\dot{\hat{\boldsymbol{W}}}_j + \sum_{j=0}^{i-1}\frac{\partial\alpha_{i-1}}{\partial\rho^{(j)}}\rho^{(j+1)} + \sum_{j=0}^{i-1}\frac{\partial\alpha_{i-1}}{\partial\beta^{(j)}}\beta^{(j+1)} + \frac{1}{2}\sum_{p,q=1}^{i-1}\frac{\partial^2\alpha_{i-1}}{\partial S_p\partial S_q}G_{S_p}^{\mathrm{T}}G_{S_q} + \sum_{j=1}^{i-1}\frac{\partial\alpha_{i-1}}{\partial S_j}\left(S_{j+1} + \bar{F}_{S_j}\right)$.

Similar to (27)–(28), with the aid of Young's inequality, it is not hard to obtain the following inequality holds

$$LV_i \le LV_{i-1} + Z_i^3\left(\alpha_i + H_i\right) + \frac{1}{4}Z_{i+1}^4 + \frac{3}{4}l_i^2 - \tilde{\boldsymbol{W}}_i^{\mathrm{T}}\boldsymbol{\Gamma}_i^{-1}\dot{\hat{\boldsymbol{W}}}_i \tag{38}$$

where l_i denotes a positive constant, $H_i = \bar{F}_{S_i} + \frac{3}{4}Z_i + \frac{3}{4l_i^2}Z_i\left\|\bar{G}_{S_i}\right\|^4 - L\alpha_{i-1}$. Since H_i contains unknown nonlinear terms, it will be approximated with the help of MTN. Specifically, for $\forall\bar{\varepsilon}_2 > 0$, there is a MTN as $\boldsymbol{W}_i^{\mathrm{T}}S_{m_i}(\boldsymbol{z}_i)$, such that

$$H_i = \boldsymbol{W}_i^{\mathrm{T}}S_{m_i}(\boldsymbol{z}_i) + \varepsilon_i(\boldsymbol{z}_i), \left|\varepsilon_i(\boldsymbol{z}_i)\right| \le \bar{\varepsilon}_i \tag{39}$$

where $\boldsymbol{z}_i = \left[Z_1, \dots, Z_i\right]^{\mathrm{T}}$. $\varepsilon_i(\boldsymbol{z}_i)$ represents the approximation error.

Using Young's inequality again, one has

$$Z_i^3\varepsilon_i(\boldsymbol{z}_i) \le \frac{3}{4}Z_i^4 + \frac{1}{4}\bar{\varepsilon}_i^4. \tag{40}$$

By combining (39) and (40), (38) can be described as

$$\begin{aligned} LV_i \le& LV_{i-1} + Z_i^3\left[\alpha_i + \boldsymbol{W}_i^{\mathrm{T}}S_{m_i}\right] + \frac{1}{4}Z_{i+1}^4 + \frac{3}{4}Z_i^4 \\ &+ \frac{1}{4}\bar{\varepsilon}_i^4 + \frac{3}{4}l_i^2 - \tilde{\boldsymbol{W}}_i^{\mathrm{T}}\boldsymbol{\Gamma}_i^{-1}\dot{\hat{\boldsymbol{W}}}_i. \end{aligned} \tag{41}$$

In order to achieve the proposed control objectives, the virtual control signal α_i and the adaptive law $\dot{\hat{\boldsymbol{W}}}_i$ are designed in the following forms

$$\alpha_i = -(c_i + 1)Z_i - \hat{\boldsymbol{W}}_i^{\mathrm{T}}S_{m_i} \tag{42}$$

$$\dot{\hat{\boldsymbol{W}}}_i = \boldsymbol{\Gamma}_i\left(S_{m_i}Z_i^3 - \sigma_i\hat{\boldsymbol{W}}_i\right) \tag{43}$$

where c_i and σ_i represent positive design constants.

Substituting (42)–(43) into (41), a new form of the differential operator of V_i can be described as

$$LV_i \le -\sum_{j=1}^{i}c_jZ_j^4 + \sum_{j=1}^{i}\sigma_j\tilde{\boldsymbol{W}}_j^{\mathrm{T}}\hat{\boldsymbol{W}}_j + \frac{1}{4}Z_{i+1}^4 + \sum_{j=1}^{i}\left(\frac{1}{4}\bar{\varepsilon}_j^4 + \frac{3}{4}l_j^2\right). \tag{44}$$

Step n: Construct the last candidate Lyapunov function, the specific form of which is as follows:

$$V_n = V_{n-1} + \frac{1}{4}Z_n^4 + \frac{1}{2}\tilde{\boldsymbol{W}}_n^{\mathrm{T}}\boldsymbol{\Gamma}_n^{-1}\tilde{\boldsymbol{W}}_n \tag{45}$$

where $\boldsymbol{\Gamma}_n = \boldsymbol{\Gamma}_n^{\mathrm{T}} > 0$ stands for a constant matrix. $\hat{\boldsymbol{W}}_n$ denotes the estimate of unknown parameter $\boldsymbol{W}_n$. $\tilde{\boldsymbol{W}}_n = \boldsymbol{W}_n - \hat{\boldsymbol{W}}_n$ represents the parameter estimate error.

By taking a similar approach as in (37) and combining (45), the differential operator of V_n can be indicated as

$$\begin{aligned} LV_n =& LV_{n-1} + Z_n^3\left(u + \bar{F}_{S_n} - L\alpha_{n-1}\right) \\ &+ \frac{3}{2}Z_n^2\bar{G}_{S_n}^{\mathrm{T}}\bar{G}_{S_n} - \tilde{\boldsymbol{W}}_n^{\mathrm{T}}\boldsymbol{\Gamma}_n^{-1}\dot{\hat{\boldsymbol{W}}}_n \end{aligned} \tag{46}$$

where $\bar{G}_{S_n} = G_{S_n} - \sum_{j=1}^{n-1}\frac{\partial\alpha_{n-1}}{\partial S_j}G_{S_j}$, $L\alpha_{n-1} = \sum_{j=1}^{n-1}\frac{\partial\alpha_{n-1}}{\partial\hat{\boldsymbol{W}}_j}\dot{\hat{\boldsymbol{W}}}_j + \sum_{j=0}^{n-1}\frac{\partial\alpha_{n-1}}{\partial\beta^{(j)}}\beta^{(j+1)} + \frac{1}{2}\sum_{i,j=1}^{n-1}\frac{\partial^2\alpha_{n-1}}{\partial S_i\partial S_j}G_{S_i}^{\mathrm{T}}G_{S_j} + \sum_{j=0}^{n-1}\frac{\partial\alpha_{n-1}}{\partial\rho^{(j)}}\rho^{(j+1)} + \sum_{j=1}^{n-1}\frac{\partial\alpha_{n-1}}{\partial S_j}\left(S_{j+1} + \bar{F}_{S_j}\right)$.

By taking a similar approach as in (28) and combining with (46), one has

$$LV_n \le LV_{n-1} + Z_n^3\left(u + H_n\right) + \frac{3}{4}l_n^2 - \tilde{\boldsymbol{W}}_n^{\mathrm{T}}\boldsymbol{\Gamma}_n^{-1}\dot{\hat{\boldsymbol{W}}}_n \tag{47}$$

where l_n denotes a positive constant. $H_n = \bar{F}_{S_n} + \frac{3}{4l_n^2}Z_n\left\|\bar{G}_{S_n}\right\|^4 - L\alpha_{n-1}$. Since H_i contains unknown nonlinear terms, it will be approximated with the aid of MTN. Specifically, for $\forall\bar{\varepsilon}_n > 0$, there is a MTN as $\boldsymbol{W}_n^{\mathrm{T}}S_{m_n}(\boldsymbol{z}_n)$, such that

$$H_n = \boldsymbol{W}_n^{\mathrm{T}}S_{m_n}(\boldsymbol{z}_n) + \varepsilon_n(\boldsymbol{z}_n), \left|\varepsilon_n(\boldsymbol{z}_n)\right| \le \bar{\varepsilon}_n \tag{48}$$

where $\boldsymbol{z}_n = \left[Z_1, \ldots, Z_n\right]^{\mathrm{T}}$. $\varepsilon_n(\boldsymbol{z}_n)$ represents the approximation error.

By taking a similar approach as in (40) and combining with (47)–(48), one has

$$\begin{aligned} LV_n \le& LV_{n-1} + Z_n^3\left[u + \boldsymbol{W}_n^{\mathrm{T}}S_{m_n}\right] + \frac{3}{4}Z_n^4 \\ &+ \frac{3}{4}l_n^2 - \tilde{\boldsymbol{W}}_n^{\mathrm{T}}\boldsymbol{\Gamma}_n^{-1}\dot{\hat{\boldsymbol{W}}}_n + \frac{1}{4}\bar{\varepsilon}_n^4. \end{aligned} \tag{49}$$

By substituting the inequality (44) into (49), we have

$$\begin{aligned} LV_n \le& -\sum_{j=1}^{n-1}c_jZ_j^4 + \sum_{j=1}^{n-1}\sigma_j\tilde{\boldsymbol{W}}_j^{\mathrm{T}}\hat{\boldsymbol{W}}_j + \sum_{j=1}^{n}\left(\frac{1}{4}\bar{\varepsilon}_j^4 + \frac{3}{4}l_j^2\right) \\ &+ Z_n^4 + Z_n^3u + Z_n^3\boldsymbol{W}_n^{\mathrm{T}}S_{m_n} - \tilde{\boldsymbol{W}}_n^{\mathrm{T}}\boldsymbol{\Gamma}_n^{-1}\dot{\hat{\boldsymbol{W}}}_n. \end{aligned} \tag{50}$$

In an effort to save the communication resources, the DETM is considered to be applied between the controller and the actuator. Combining the DETM (9)–(10), the virtual control signal α_n, the adaptive law $\hat{\boldsymbol{W}}_n$ and $\varpi(t)$ are designed as follows:

$$\alpha_n = -(c_n+1)Z_n - \hat{\boldsymbol{W}}_n^{\mathrm{T}}S_{m_n} \tag{51}$$

$$\dot{\hat{\boldsymbol{W}}}_n = \boldsymbol{\Gamma}_n\left(S_{m_n}Z_n^3 - \sigma_n\hat{\boldsymbol{W}}_n\right) \tag{52}$$

$$\varpi(t) = \alpha_n - (\iota+\varsigma)\tanh\left(\frac{Z_n^3(\iota+\varsigma)}{\delta}\right) \tag{53}$$

where c_n, δ and σ_n are positive design constants. ι and ς are already defined in (10).

According to the DETM (9)–(10), for $\forall t \in \left[t_k, t_{k+1}\right)$, we have $|\varrho(t)| = |u(t) - \varpi(t)| < \iota+\varsigma \le |\iota+\varsigma|$. Based on (51)–(53) and Lemma 1, one has

$$\begin{aligned} Z_n^3u \le& Z_n^3\left[|u - \varpi(t)| + \varpi(t)\right] \\ \le& \left|Z_n^3(\iota+\varsigma)\right| - Z_n^3(\varsigma+\iota)\tanh\left(\frac{Z_n^3(\varsigma+\iota)}{\delta}\right) + Z_n^3\alpha_n \\ \le& 0.2785\delta - (c_n+1)Z_n^4 - Z_n^3\hat{\boldsymbol{W}}_n^{\mathrm{T}}S_{m_n}. \end{aligned} \tag{54}$$

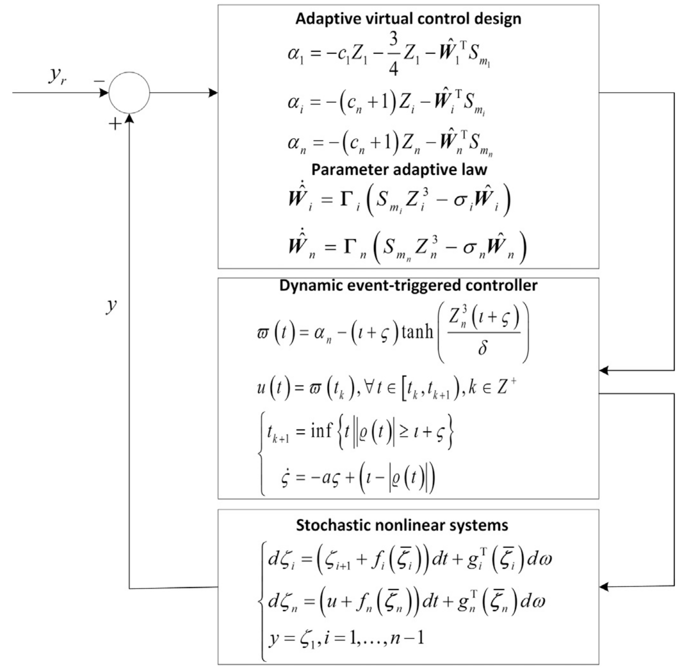

Fig. 1. The block diagram of control process.

By substituting (52) and (54) into (50), a new form of the differential operator of V_n can be indicated as

$$LV_n \le -\sum_{j=1}^{n}c_jZ_j^4 + \sum_{j=1}^{n}\sigma_j\tilde{\boldsymbol{W}}_j^{\mathrm{T}}\hat{\boldsymbol{W}}_j + \sum_{j=1}^{n}\left(\frac{1}{4}\bar{\varepsilon}_j^4 + \frac{3}{4}l_j^2\right) + 0.2785\delta. \tag{55}$$

With a view to improving the clarity, the block diagram of control process is shown in Fig. 1.

Theorem 1. *For the controlled stochastic system (1) with dynamic event-triggered mechanism (9)–(10), if Assumption 1 is satisfied, let the virtual control laws be designed as (33), (42) and (51), and the adaptive laws be chosen as (34), (43) and (52), it holds*

(i) All signals of the controlled system (1) realize the SGUUB in the sense of 4th moment.

(ii) After the preassigned time T_p, all states adhere to the constraint boundary conditions no matter what the initial value conditions are, and the tracking error satisfies the pregiven performance constraints.

(iii) The Zeno phenomenon does not happen.

Proof. At first, the Lyapunov function is selected as

$$V = V_n = \sum_{j=1}^{n}\left(\frac{1}{4}Z_j^4 + \frac{1}{2}\tilde{\boldsymbol{W}}_j^{\mathrm{T}}\boldsymbol{\Gamma}_j^{-1}\tilde{\boldsymbol{W}}_j\right). \tag{56}$$

(i) According to (56), one has $LV = LV_n$. By using Young's inequality, the term $\sum_{j=1}^{n}\sigma_j\tilde{\boldsymbol{W}}_j^{\mathrm{T}}\hat{\boldsymbol{W}}_j$ in (55) can be expressed as

$$\sum_{j=1}^{n}\sigma_j\tilde{\boldsymbol{W}}_j^{\mathrm{T}}\hat{\boldsymbol{W}}_j \le -\sum_{j=1}^{n}\frac{\sigma_j}{2\lambda_{\max}\left(\boldsymbol{\Gamma}_j^{-1}\right)}\tilde{\boldsymbol{W}}_j^{\mathrm{T}}\boldsymbol{\Gamma}_j^{-1}\tilde{\boldsymbol{W}}_j + \frac{1}{2}\sum_{j=1}^{n}\sigma_j\left\|\boldsymbol{W}_j\right\|^2 \tag{57}$$

where $\lambda_{\max}\left(\boldsymbol{\Gamma}_j^{-1}\right)$ represents the maximum eigenvalue of $\boldsymbol{\Gamma}_j^{-1}$.

Clearly, by substituting (57) into (55) and considering the definition of V in (56), the differential operator of V can be described in the following form

$$\begin{aligned} LV \le & -\sum_{j=1}^{n} c_j Z_j^4 - \frac{1}{2}\sum_{j=1}^{n} \frac{\sigma_j}{\lambda_{\max}\left(\boldsymbol{\Gamma}_j^{-1}\right)} \tilde{\boldsymbol{W}}_j^{\mathrm{T}} \boldsymbol{\Gamma}_j^{-1} \tilde{\boldsymbol{W}}_j + \frac{1}{2}\sum_{j=1}^{n} \sigma_j \left\| \boldsymbol{W}_j \right\|^2 \\ & + \sum_{j=1}^{n} \left(\frac{1}{4}\bar{\varepsilon}_j^4 + \frac{3}{4} l_j^2 \right) + 0.2785\delta \\ \le & -bV + \Xi \end{aligned} \tag{58}$$

where $b = \min\left\{4c_i, \sigma_i / \left(\lambda_{\max}\left(\boldsymbol{\Gamma}_i^{-1}\right)\right), i = 1, \ldots, n\right\}$, $\Xi = \sum_{j=1}^{n}\left(\frac{1}{4}\bar{\varepsilon}_j^4 + \frac{3}{4}l_j^2\right) + 0.2785\delta + \frac{1}{2}\sum_{j=1}^{n}\sigma_j \left\|\boldsymbol{W}_j\right\|^2$.

According to (58) and Lemma 2, we have

$$E[V] \le V(\mathbf{0})e^{-bt} + \frac{\Xi}{b} \le V(\mathbf{0}) + \frac{\Xi}{b}. \tag{59}$$

where $V(\mathbf{0}) = \sum_{j=1}^{n}\left[\frac{1}{4}Z_j^4(\mathbf{0}) + \frac{1}{2}\tilde{\boldsymbol{W}}_j^{\mathrm{T}}(\mathbf{0})\,\boldsymbol{\Gamma}_j^{-1}\tilde{\boldsymbol{W}}_j(\mathbf{0})\right]$.

Based on (56) and (59), we get

$$\sum_{i=1}^{n} E\left[\left\|Z_i\right\|^4\right] \le 4E\left[V(\mathbf{0})\right] + \frac{4\Xi}{b}. \tag{60}$$

Therefore, according to Lemma 2 and Definition 2, it is not difficult to conclude that all signals of the controlled system (1) realize the SGUUB attribute in the sense of 4th moment.

(ii) Based on (60) and $Z_1 = S_1$, one has

$$E\left[\left\|S_1\right\|^2\right] \le \sqrt{4E\left[V(0)\right] + \frac{4\Xi}{b}}. \tag{61}$$

When $t \ge T_p$, $\beta(t) = 1$, based on (16), we can obtain $E\left[\left\|e_1\right\|\right] \le |\varphi|$. This shows that the tracking error e_1 satisfies the pregiven performance constraints. Moreover, using the similar analysis in [28], it can be proved all states adhere to the constraint boundary conditions after the preassigned time T_p.

(iii) It needs to be proved that for $\forall k \in Z^+$, there exists a time constant $t^* > 0$ such that $\left\{t_{k+1} - t_k\right\} \ge t^*$. From (53), $\dot{\varpi}(t)$ is a continuous and bounded function, so there exists a positive constant $\upsilon > 0$ which makes $|\dot{\varpi}(t)| \le \upsilon$. Based on $\varrho(t) = \varpi(t) - u(t)$, we can get $\frac{d\varrho(t)}{dt} \le |\dot{\varrho}(t)| \le |\dot{\varpi}(t)| \le \upsilon$. By considering $\varrho\left(t_k\right) = 0$ and $\lim_{t\to t_{k+1}}\varrho(t) = \varsigma + \imath > 0$, we know that the lower bound of the inter-execution interval t^* must satisfy $t_{k+1} - t_k \ge t^* = (\varsigma + \imath)/\upsilon$. As a result, the Zeno phenomenon is successfully prevented.

As shown above, the proof of Theorem 1 is completed.

4. Simulation example

To verify the merits of the proposed control scheme, a numerical simulation example and a practical simulation example are taken into account in the section.

Example 1. Consider a second-order stochastic system with the following mathematical expression:

$$\begin{cases} d\zeta_1 = \left(\zeta_2 - 0.1\sin\left(\zeta_1^2\right)\right)dt + 0.1\sin(\zeta_1)d\omega \\ d\zeta_2 = (u - \zeta_1^2 - 0.1\sin(\zeta_2))dt + 0.01\sin(\zeta_1\zeta_2)d\omega \\ y = \zeta_1 \end{cases} \tag{62}$$

In the simulation, the expectation signal is chosen as $y_r = 0.5\sin(t) - 1$. The initial state values are chosen as $\zeta_1(0) = 0$ and $\zeta_2(0) = 0$. The preassigned time is selected as $T_p = 3$. All design parameters are assigned as $c_1 = 10$, $c_2 = 5$, $\Gamma_1 = 7\boldsymbol{I}_5$, $\Gamma_2 = 2\boldsymbol{I}_9$, $a = 0.3$, $\imath = 0.1$, $\sigma_1 = 11$, $\sigma_2 = 10$, $\delta = 3$, $\varphi_0 = 9.5$ and $\varphi_1 = 0.2$.

The simulation results are presented in Table 1 and Figs. 2–6. As can be seen from Table 1, the number of triggered events for DETM is less than that for ETM in [43], which indicates DETM can save communication resources more effectively. Fig. 2 displays the trajectories of system outputs and the tracking errors under two types of ETMs. It is apparent that DETM and ETM in [43] achieve similar tracking effects. Specifically, the output signals ζ_1 with DETM and ETM in [43] both satisfy the given asymmetric time-varying constraints after the preassigned time T_p, while their initial values violate the given constraints. Additionally, the tracking errors satisfy the pregiven performance constraint. Fig. 3 illustrates the trajectory of system state ζ_2, which shows that ζ_2 satisfies the given symmetric time-varying constraints after the preassigned time T_p. Fig. 4 displays the variation of the dynamic parameter ς under DETM. Fig. 5 shows that the time interval between events with DETM is greater than zero, which confirms that Zeno behavior has been effectively avoided. In addition, the control signals $u(t)$ and $\varpi(t)$ with DETM are plotted in Fig. 6.

Table 1
Comparison of two ETMs.

	t = 20	t = 30	t = 35
DETM	1905	2666	3016
ETM in [43]	2429	3778	4351

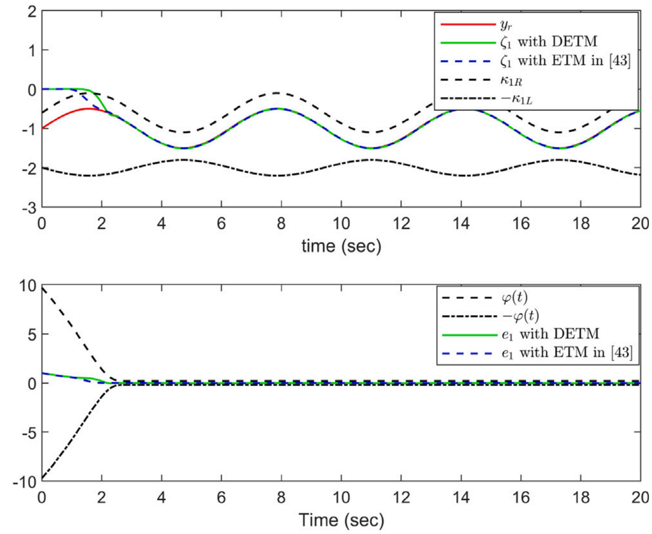

Fig. 2. System outputs and tracking errors under two ETMs.

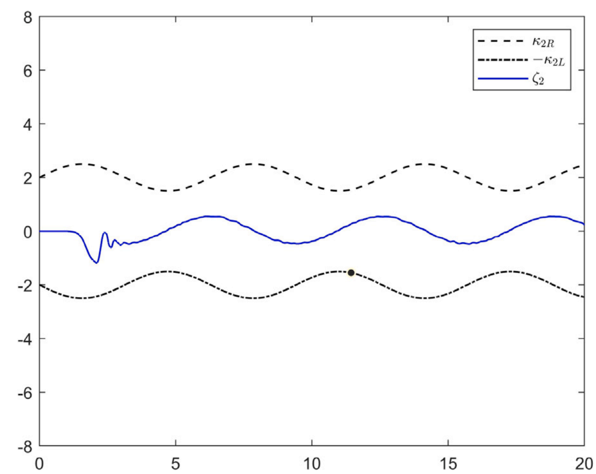

Fig. 3. The trajectory of ζ_2 with DETM.

Example 2. To further substantiate the efficacy and applicability of the proposed control scheme, the single-link robot arm system [47] is considered.

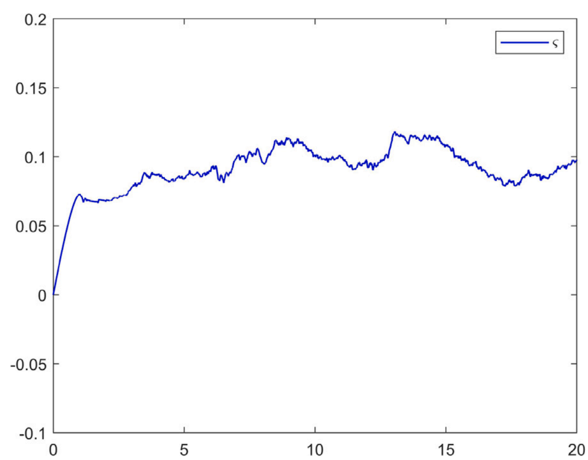

Fig. 4. The trajectory of ς with DETM.

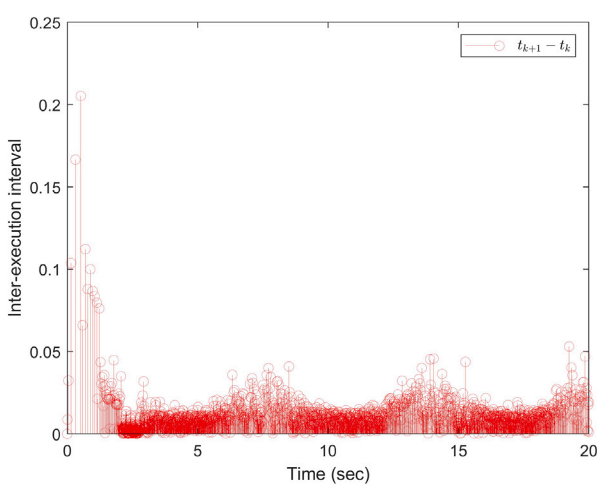

Fig. 5. Time interval of triggering events with DETM.

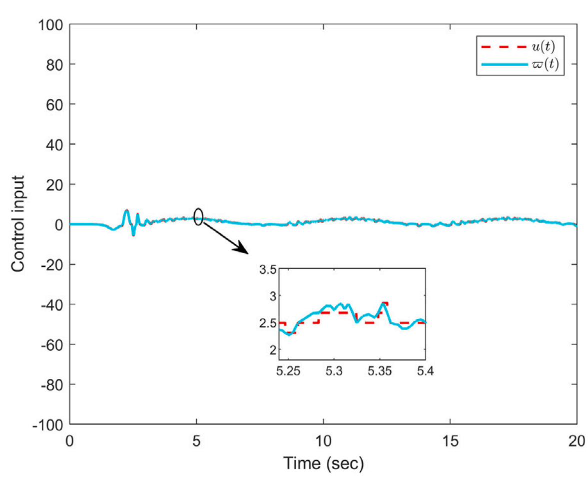

Fig. 6. The controller $\varpi(t)$ and actuator $u(t)$ with DETM.

The dynamic model of the single-link robot arm system is shown as follows:

$$R\ddot{q} + D\dot{q} + Mlg\sin(q) = u \tag{63}$$

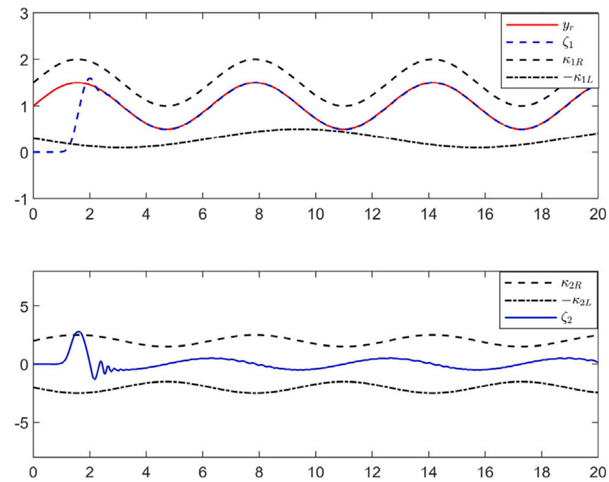

Fig. 7. The trajectories of system states with deferred constraints.

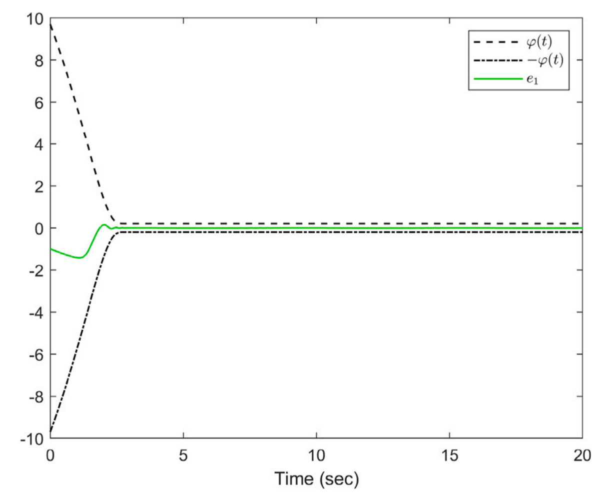

Fig. 8. The tracking error with performance constraints.

where q, $\dot{q}$ and $\ddot{q}$ denote the link angular displacement, velocity and acceleration, respectively. u denotes the system input, R represents the torque of inertia. D and g are the damping coefficient and the acceleration of gravity, respectively. l and M denote the link length and the object mass, respectively.

Since stochastic noise is unavoidable in real-world situations, the single-link robot systems with stochastic perturbations is taken into consideration. Define $\zeta_1 = q$ and $\zeta_2 = \dot{q}$, (63) can be converted into the following system:

$$\begin{cases} d\zeta_1 = \zeta_2 dt \\ d\zeta_2 = R^{-1}(u - D\zeta_2 - Mlg\sin(\zeta_1))dt + g_2 d\omega \\ \quad y = \zeta_1 \end{cases} \tag{64}$$

where $g_2 = \zeta_1\zeta_2$. $R = 1\ kg{\cdot}m^2$, $g = 10N/kg$. D, M and l denote unknown design parameters.

In the simulation, the expectation signal is chosen as $y_r = 0.5\sin(t) + 1$. The initial state values are chosen as $\zeta_1(0) = 0$ and $\zeta_2(0) = 0$. The preassigned time is selected as $T_p = 3$. All design parameters are assigned as $c_1 = 20$, $c_2 = 5$, $\Gamma_1 = 7\boldsymbol{I}_5$, $\Gamma_2 = 7\boldsymbol{I}_9$, $a = 0.3$, $M = 1$, $D = 0.5$, $l = 0.1$, $\iota = 0.1$, $\sigma_1 = 11$, $\sigma_2 = 10$, $\delta = 3$, $\varphi_0 = 9.5$ and $\varphi_1 = 0.2$.

The simulation results are presented in Figs. 7–10. From Fig. 7, it is easy to known that all of the system states violate the given constraints when $t \in [0, T_p)$ and they satisfy the given time-varying constraints after the preassigned time T_p. Fig. 8 shows the tracking error e_1 meets

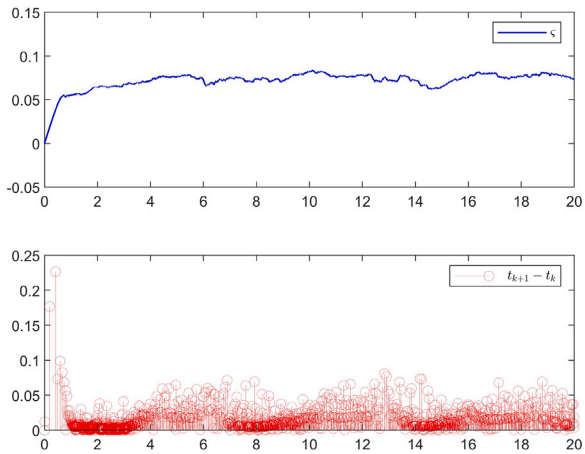

Fig. 9. The trajectory of ς and time interval of triggering events.

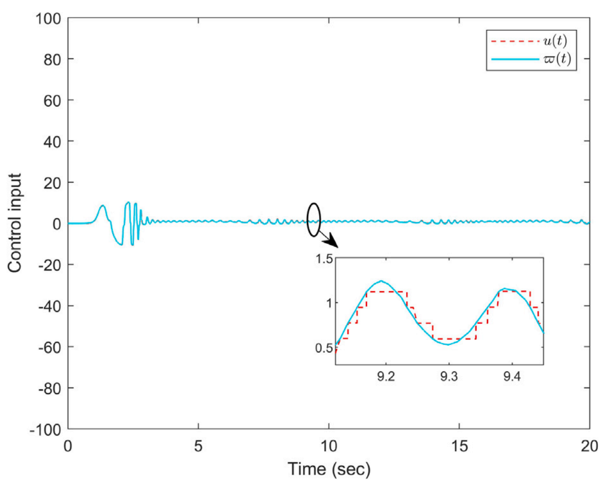

Fig. 10. The controller $\varpi(t)$ and actuator $u(t)$.

the pregiven performance constraint, which also implies a satisfactory tracking result is obtained. Fig. 9 demonstrates the variation of the dynamic parameter ς and the time interval between events is greater than zero, which confirms that Zeno behavior has been avoided successfully. Fig. 10 displays the trajectories of control signals $u(t)$ and $\varpi(t)$.

Remark 4. In the two simulation examples in this article, the deferred symmetric and asymmetric full-state time-varying constraints on the stochastic system are considered. There are three types of the state boundary functions that are considered, they are all positive, one positive and one negative, and all negative Moreover, satisfactory simulation results are obtained, which means the control scheme proposed in this article is effective.

5. Conclusion

In this article, a DETM-based adaptive tracking control scheme has been proposed for stochastic nonlinear systems with deferred time-varying constraints. Firstly, the novel UUBF and deferred funnel error transformation have been developed to deal with different types of state constraints and adjust the tracking error, respectively. The unknown nonlinear terms have been approximated with the use of MTN. The DETM has been introduced to design controller, which can ensure that all the signals of the controlled system are SGUUB in the sense of 4th moment while conserving more communication resources. The proposed control scheme can achieve that all system states strictly obey the pregiven boundary constraints and the tracking error converges to a prescribed region after the preassigned time. Moreover, the preassigned time can be set according to practical requirements. Two simulation examples have verified the effectiveness and wide applicability of the proposed control scheme. For future investigation, more efforts can be made in prescribed-time output-feedback control for stochastic nonlinear multiagent systems with deferred constraints.

CRediT authorship contribution statement

Dong-Mei Wang: Writing – original draft, Software, Formal analysis. **Yu-Qun Han:** Writing – review & editing, Supervision, Methodology. **Li-Ting Lu:** Writing – original draft, Methodology. **Shan-Liang Zhu:** Writing – review & editing, Supervision, Methodology, Formal analysis.

Declaration of competing interest

The authors declare that they have no known competing financial interests or personal relationships that could have appeared to influence the work reported in this paper.

Data availability

No data was used for the research described in the article.

References

[1] Xu YJ, Xin M. Nonlinear stochastic control for space launch vehicles. IEEE Trans Aerosp Electron Syst 2011;47(1):98–108. http://dx.doi.org/10.1109/TAES.2011.5705662.

[2] Diwekar UM, Rubin ES. Stochastic modeling of chemical processes. Comput Chem Eng 1991;15(2):105–14. http://dx.doi.org/10.1016/0098-1354(91)87009-X.

[3] Gao YF, Sun XM, Wen CY, Wang W. Adaptive tracking control for a class of stochastic uncertain nonlinear systems with input saturation. IEEE Trans Automat Control 2017;62(5):2498–504. http://dx.doi.org/10.1109/TAC.2016.2600340.

[4] Ji HB, Xi HS. Adaptive output-feedback tracking of stochastic nonlinear systems. IEEE Trans Automat Control 2006;51(2):355–60. http://dx.doi.org/10.1109/TAC.2005.863501.

[5] Liu SJ, Zhang JF, Jiang ZP. Decentralized adaptive output-feedback stabilization for large-scale stochastic nonlinear systems. Automatica 2007;43(2):238–51. http://dx.doi.org/10.1016/j.automatica.2006.08.028.

[6] Tong SC, Wang T, Li YM. Fuzzy adaptive actuator failure compensation control of uncertain stochastic nonlinear systems with unmodeled dynamics. IEEE Trans Fuzzy Syst 2014;22(3):563–74. http://dx.doi.org/10.1109/TFUZZ.2013.2264939.

[7] Wang F, Chen B, Sun YM, Gao YL, Lin C. Finite-time fuzzy control of stochastic nonlinear systems. IEEE Trans Cybern 2020;50(6):2617–26. http://dx.doi.org/10.1109/TCYB.2019.2925573.

[8] Wu J, Chen XM, Zhao QJ, Li J, Wu ZG. Adaptive neural dynamic surface control with prespecified tracking accuracy of uncertain stochastic nonstrict-feedback systems. IEEE Trans Cybern 2022;52(5):3408–21. http://dx.doi.org/10.1109/TCYB.2020.3012607.

[9] Han YQ. Design of decentralized adaptive control approach for large-scale nonlinear systems subjected to input delays under prescribed performance. Nonlinear Dynam 2021;106(1):565–82. http://dx.doi.org/10.1007/s11071-021-06843-z.

[10] Sun YM, Chen B, Lin C, Wang HH, Zhou SW. Adaptive neural control for a class of stochastic nonlinear systems by backstepping approach. Inform Sci 2016;369:748–64. http://dx.doi.org/10.1016/j.ins.2016.06.010.

[11] Zhao XD, Wang XY, Zong GD, Zheng XL. Adaptive neural tracking control for switched high-order stochastic nonlinear systems. IEEE Trans Cybern 2017;47(10):3088–99. http://dx.doi.org/10.1109/TCYB.2017.2684218.

[12] Wu J, Wang W, Ding SH, Xie XP, Yi Y. Adaptive neural optimized control for uncertain strict-feedback systems with unknown control directions and pre-set performance. Commun Nonlinear Sci Numer Simul 2023;126:107506. http://dx.doi.org/10.1016/j.cnsns.2023.107506.

[13] Liu YL, Ma HJ. Adaptive fuzzy tracking control of nonlinear switched stochastic systems with prescribed performance and unknown control directions. IEEE Trans Syst Man Cybern 2020;50(2):590–9. http://dx.doi.org/10.1109/TSMC.2017.2764685.

[14] Liu Y, Zhang HG, Wang YC, Ren H, Li QC. Adaptive fuzzy prescribed finite-time tracking control for nonlinear system with unknown control directions. IEEE Trans Fuzzy Syst 2022;30(6):1993–2003. http://dx.doi.org/10.1109/TFUZZ.2021.3072696.

[15] He WJ, Zhu SL, Lu LT, Zhao W, Han YQ. Adaptive multi-switching-based global tracking control for switched nonlinear systems with prescribed performance. IEEE Trans Autom Sci Eng 2023. http://dx.doi.org/10.1109/TASE.2023.3277470.

[16] He WJ, Zhu SL, Li N, Han YQ. Adaptive finite-time control for switched nonlinear systems subject to multiple objective constraints via multi-dimensional Taylor network approach. ISA Trans 2023;136:323–33. http://dx.doi.org/10.1016/j.isatra.2022.10.048.

[17] Wang MX, Zhu SL, Liu SM, Du Y, Han YQ. Design of adaptive finite-time fault-tolerant controller for stochastic nonlinear systems with multiple faults. IEEE Trans Autom Sci Eng 2023;20(4):2492–502. http://dx.doi.org/10.1109/TASE.2022.3206328.

[18] Yan HS, Wang GB. Adaptive tracking control for stochastic nonlinear systems with time-varying delays using multi-dimensional Taylor network. ISA Trans 2023;132:246–57. http://dx.doi.org/10.1016/j.isatra.2022.06.004.

[19] Wang GB, Yan HS. Contraction-based model predictive control for stochastic nonlinear discrete-time systems with time-varying delays via multi-dimensional Taylor network. J Franklin Inst B 2023;360(3):1613–34. http://dx.doi.org/10.1016/j.jfranklin.2022.12.024.

[20] Yu XB, He W, Li HY, Sun J. Adaptive fuzzy full-state and output-feedback control for uncertain robots with output constraint. IEEE Trans Syst Man Cybern 2021;51(11):6994–7007. http://dx.doi.org/10.1109/TSMC.2019.2963072.

[21] Jia FL, He X. Fault-tolerant control for uncertain nonstrict-feedback stochastic nonlinear systems with output constraints. IEEE Trans Syst Man Cybern 2023;53(8):5212–23. http://dx.doi.org/10.1109/TSMC.2023.3260583.

[22] Ma L, Mei KQ, Ding SH, Pan TH. Design of adaptive fuzzy fixed-time HOSM controller subject to asymmetric output constraints. IEEE Trans Fuzzy Syst 2023;31(9):2989–99. http://dx.doi.org/10.1109/TFUZZ.2023.3241147.

[23] Zhang S, Dong YT, Ou Yang YC, Yin Z, Peng KX. Adaptive neural control for robotic manipulators with output constraints and uncertainties. IEEE Trans Neural Netw Learn Syst 2018;29(11):5554–64. http://dx.doi.org/10.1109/TNNLS.2018.2803827.

[24] Li DP, Li DJ. Adaptive neural tracking control for an uncertain state constrained robotic manipulator with unknown time-varying delays. IEEE Trans Syst Man Cybern 2018;48(12):2219–28. http://dx.doi.org/10.1109/TSMC.2017.2703921.

[25] Liu YJ, Lu SM, Tong SC, Chen XK, Chen CLP, Li DJ. Adaptive control-based Barrier Lyapunov Functions for a class of stochastic nonlinear systems with full state constraints. Automatica 2018;87:83–93. http://dx.doi.org/10.1016/j.automatica.2017.07.028.

[26] Wu ZH, Zheng SP, Zhao YJ, Liu BJ, Ni JK. Fixed-time composite neural learning control of state-constrained nonlinear uncertain systems. J Franklin Inst B 2021;358(16):8138–68. http://dx.doi.org/10.1016/j.jfranklin.2021.08.013.

[27] Jin X, Li YX. Adaptive fuzzy control of uncertain stochastic nonlinear systems with full state constraints. Inform Sci 2021;574:625–39. http://dx.doi.org/10.1016/j.ins.2021.07.056.

[28] Song YD, Zhou SY. Tracking control of uncertain nonlinear systems with deferred asymmetric time-varying full state constraints. Automatica 2018;98:314–22. http://dx.doi.org/10.1016/j.automatica.2018.09.032.

[29] Yang B, Cao L, Xiao WB, Yao DY, Lu RQ. Event-triggered adaptive neural control for multiagent systems with deferred state constraints. J Syst Sci Complex 2022;35(3):973–92. http://dx.doi.org/10.1007/s11424-021-0201-6.

[30] Zhao K, Chen L, Chen CLP. Event-based adaptive neural control of nonlinear systems with deferred constraint. IEEE Trans Syst Man Cybern 2022;52(10):6273–82. http://dx.doi.org/10.1109/TSMC.2022.3143359.

[31] Wu J, He FR, Shen H, Ding SH, Wu ZG. Adaptive NN fixed-time fault-tolerant control for uncertain stochastic system with deferred output constraint via self-triggered mechanism. IEEE Trans Cybern 2023;53(9):5892–903. http://dx.doi.org/10.1109/TCYB.2022.3205765.

[32] Guo XY, Zhang HG, Sun JY, Liu X. Cooperative control for stochastic multiagent systems with deferred dynamic constraints via a novel universal barrier function approach. IEEE Trans Cybern 2024;54(3):1806–15. http://dx.doi.org/10.1109/TCYB.2023.3259967.

[33] Åström KJ, Bernhardsson B. Comparison of periodic and event based sampling for first-order stochastic systems. IFAC Proc Vol 1999;32(2):5006–11. http://dx.doi.org/10.1016/S1474-6670(17)56852-4.

[34] Chen HY, Zong GD, Zhao XD, Gao FZ, Shi KB. Secure filter design of fuzzy switched CPSs with mismatched modes and application: A multidomain event-triggered strategy. IEEE Trans Ind Inf 2023;19(10):10034–44. http://dx.doi.org/10.1109/TII.2022.3232768.

[35] Liu L, Li XS. Event-triggered tracking control for active seat suspension systems with time-varying full-state constraints. IEEE Trans Syst Man Cybern 2022;52(1):582–90. http://dx.doi.org/10.1109/TSMC.2020.3003368.

[36] Ma H, Li HY, Liang HJ, Dong GW. Adaptive fuzzy event-triggered control for stochastic nonlinear systems with full state constraints and actuator faults. IEEE Trans Fuzzy Syst 2019;27(11):2242–54. http://dx.doi.org/10.1109/TFUZZ.2019.2896843.

[37] Xing LT, Wen CY, Liu ZT, Su HY, Cai JP. Event-triggered adaptive control for a class of uncertain nonlinear systems. IEEE Trans Automat Control 2017;62(4):2071–6. http://dx.doi.org/10.1109/TAC.2016.2594204.

[38] Girard A. Dynamic triggering mechanisms for event-triggered control. IEEE Trans Automat Control 2015;60(7):1992–7. http://dx.doi.org/10.1109/TAC.2014.2366855.

[39] Chen MS, Yan HC, Zhang H, Chi M, Li ZC. Dynamic event-triggered asynchronous control for nonlinear multiagent systems based on T–S fuzzy models. IEEE Trans Fuzzy Syst 2021;29(9):2580–92. http://dx.doi.org/10.1109/TFUZZ.2020.3004009.

[40] Sun JK, Yang J, Li SH, Zheng WX. Output-based dynamic event-triggered mechanisms for disturbance rejection control of networked nonlinear systems. IEEE Trans Cybern 2020;50(5):1978–88. http://dx.doi.org/10.1109/TCYB.2018.2877413.

[41] Shu F, Zhai JY. Dynamic event-triggered tracking control for a class of p-normal nonlinear systems. IEEE Trans Circuits Syst I Regul Pap 2021;68(2):808–17. http://dx.doi.org/10.1109/TCSI.2020.3036367.

[42] Fu YY, Li J, Li XB, Wu SY. Dynamic event-triggered adaptive control for uncertain stochastic nonlinear systems. Appl Math Comput 2023;444:127800. http://dx.doi.org/10.1016/j.amc.2022.127800.

[43] Qiu JB, Ma M, Wang T. Event-triggered adaptive fuzzy fault-tolerant control for stochastic nonlinear systems via command filtering. IEEE Trans Syst Man Cybern 2022;52(2):1145–55. http://dx.doi.org/10.1109/TSMC.2020.3013744.

[44] Hua CC, Ning PJ, Li K, Guan XP. Fixed-Time prescribed tracking control for stochastic nonlinear systems with unknown measurement sensitivity. IEEE Trans Cybern 2022;52(5):3722–32. http://dx.doi.org/10.1109/TCYB.2020.3012560.

[45] Liu Y, Liu XP, Jing YW. Adaptive neural networks finite-time tracking control for non-strict feedback systems via prescribed performance. Inform Sci 2018;468:29–46. http://dx.doi.org/10.1016/j.ins.2018.08.029.

[46] Li DP, Liu L, Liu YJ, Tong SC, Chen CLP. Adaptive NN control without feasibility conditions for nonlinear state constrained stochastic systems with unknown time delays. IEEE Trans Cybern 2019;49(12):4485–94. http://dx.doi.org/10.1109/TCYB.2019.2903869.

[47] He M, Li JM. Event-triggered adaptive tracking control for a class of uncertain stochastic nonlinear systems with Markov jumping parameters. Internat J Adapt Control Signal Process 2018;32(12):1655–74. http://dx.doi.org/10.1002/acs.2936.